

# Temperature and pH driven association in uranyl aqueous solutions

M. Druchok, M. Holovko

Institute for Condensed Matter Physics, NAS of Ukraine, 1 Svientsitskii St., 79011 Lviv, Ukraine

Received July 3, 2012, in final form September 19, 2012

An association behavior of uranyl ions in aqueous solutions is explored. For this purpose a set of all-atom molecular dynamics simulations is performed. During the simulation, the fractions of uranyl ions involved in dimer and trimer formations were monitored. To accompany the fraction statistics one also collected distributions characterizing average times of the dimer and trimer associates. Two factors effecting the uranyl association were considered: temperature and pH. As one can expect, an increase of the temperature decreases an uranyl capability of forming the associates, thus lowering bound fractions/times and vice versa. The effect of pH was modeled by adding  $H^+$  or  $OH^-$  ions to a “neutral” solution. The addition of hydroxide ions  $OH^-$  favors the formation of the associates, thus increasing bound times and fractions. The extra  $H^+$  ions in a solution produce an opposite effect, thus lowering the uranyl association capability. We also made a structural analysis for all the observed associates to reveal the mutual orientation of the uranyl ions.

**Key words:** molecular dynamics, uranyl aqueous solution, association, pH, temperature

**PACS:** 61.20.Ja, 61.20.Qg, 82.20.Wt, 82.30.Hk, 82.30.Nr

## 1. Introduction

For the last decades, the unresolved problem of nuclear fuel wastes containing actinides and other radionuclides contacting with water urged intensive theoretical and experimental studies. Comprehension of the association processes in such systems can provide one with important data for chemical technology, medicine, environmental ecology [1]. The actinides An in water can easily form dioxides called actynils  $(AnO_2)^{2+}$ . Both An=O bond lengths are usually 1.7–1.8 Å and O=An=O angle is close to 180°. Actynil is usually hydrated by five water molecules, the so-called ligands, located in an equatorial plane (normal to O=An=O axis) at the distances of 2.5–2.6 Å. Such a finding was confirmed by quantum-chemical investigations. In particular, in [2, 3] it is shown that the number of ligands of uranyl, neptunyl and plutonyl is equal to five. It was also found that a hydrolysis reaction with one proton loss from one of five uranyl ligands is energetically favorable. However, the quantum-chemical calculations cannot provide a scrupulous understanding of the role of the surroundings beyond the hydrated-hydrolyzed complex, which is essential for a correct interpretation of many structural, dynamic, and thermodynamic properties of these complexes [4]. In [5–7], the molecular dynamics simulations were carried out for aqueous solutions of actinides using rigid TIP3P or SPC water models. Neither the deformation of water molecules nor the hydrolysis effects in a hydration shell were possible due to constrained rigid models of water molecules. No hydrolysis evidence was also found in a recent investigation of uranyl hydration by the *ab initio* molecular dynamics simulation [8].

In computer simulations, in order to explicitly treat the cation hydrolysis effect, water should be considered in the framework of a non-constrained flexible model. In our previous studies [9–13], water was treated within a slightly modified version of central force model CF1 [14, 15]. It was found that with an increase of the cation-water interaction, some water molecules in the cation hydration shell lost some protons. This effect was treated as the hydrolysis of water caused by a high valency of the cation. In [13, 16], the CF1 model for water was also used for the investigation of the hydration structure of the

uranyl ion  $\text{UO}_2^{2+}$ . It is found that the uranyl hydration shell has bipyramidal pentacoordinated structure with five ligands. It includes four water molecules and one hydroxide  $\text{OH}^-$  ion. Usually the cation hydrolysis process does not stop at the creation of the hydrated-hydrolyzed complexes and proceeds to a condensation reaction creating polynuclear ions [17].

Apparently, the tendency for the cation hydrolysis depends on the pH of an aqueous solution. One can expect a hydrolysis effect in an alkaline solution stronger than in an acidic one. Some previous results for the computer modeling of the effect of pH on the cation hydrolysis of an uranyl ion  $\text{UO}_2^{2+}$  were presented in [13]. In this paper we continue the investigation of the formation of the ionic associates between uranyl ions. In particular, we study the effect of the temperature and pH of an aqueous solution on the structure of the uranyl dimers and trimers.

## 2. Model and method

Three different solutions are considered. The first one is a solution with 1600 water molecules and 16 uranyl ions. To mimic an acidic or alkaline conditions, we add 100  $\text{H}^+$  or 100  $\text{OH}^-$  ions to the initial “neutral” solution, respectively. For simplicity we will further refer to these solutions as alkaline, neutral, and acidic.

The model is similar to the one used in our study of the uranyl hydration [16]. Central force model CF1 was engaged in water description. For the uranyl-water interaction we took the potentials from [7]. These potentials are of the “1–12–6” type:

$$E_{ij} = \frac{Z_i Z_j}{4\pi\epsilon_0 r} + \frac{A_i A_j}{r^{12}} - \frac{B_i B_j}{r^6}. \quad (2.1)$$

The corresponding potential parameters are listed in table 1.

**Table 1.** Potential parameters for uranyl-water interaction.

	Z	A (kcal $\text{\AA}^{12}/\text{mol})^{1/2}$	B (kcal $\text{\AA}^6/\text{mol})^{1/2}$
O in $\text{H}_2\text{O}$	-0.65966	793.322	25.010
H	0.32983	0.1	0.0
U	2.50	629.730	27.741
O in $\text{UO}_2$	-0.25	793.322	25.010

In order to preserve the uranyl intramolecular geometry, additional constraints are used for the U=O bond length in the form  $E_{ij} \sim (r - 1.75)^2$  and for the O=U=O angle in the form  $E_{ij} \sim (\theta - 180)^2$ . The distances are measured in  $\text{\AA}$ , the angles – in degrees, the energies – in kcal/mol.

All the species were allowed to move freely across the MD cell. The cut-off radius for the short-range interactions is chosen to be 15  $\text{\AA}$ . The long-range Coulomb interactions were taken into account by the Ewald summation technique. One has to note that all the systems considered are physically non-neutral but still can be effectively treated because the charges are implicitly compensated by a neutralizing background in the Ewald formulation. The pressure (1 bar) and the temperature (278 K or 318 K) were controlled by means of a Nose-Hoover barostat and thermostat in an isotropic  $NPT$  ensemble [18, 19]. The particles were placed into a cubic box ( $L_x = L_y = L_z \approx 37 \text{\AA}$ ) with periodic boundary conditions. The length of the production runs ranged from 7 to 10 ns. As before [10–13], we used the velocity Verlet algorithm with a time step 0.2 fs to integrate the classical equations of motion.

For structural analysis, the radial distribution functions (RDFs) are collected. The angular distributions of uranyl-uranyl mutual orientation are also accumulated during the simulations. To accompany structural details, we have also collected distributions of lifetimes of the uranyl dimers and trimers.

### 3. Numerical results

In this section we present the results of the simulations. It includes the RDFs describing the uranyl-solution and uranyl-uranyl correlation. As it is mentioned above, we also collected angular distributions. Further we discuss distributions of lifetimes of the uranyl dimers and trimers.

#### 3.1. Radial distribution functions

In figure 1 we present the RDFs for the uranium-oxygen correlation for  $T = 278$  K (left hand panel) and 318 K (right hand panel). The red solid lines denote the results for the alkaline, the green dashed lines

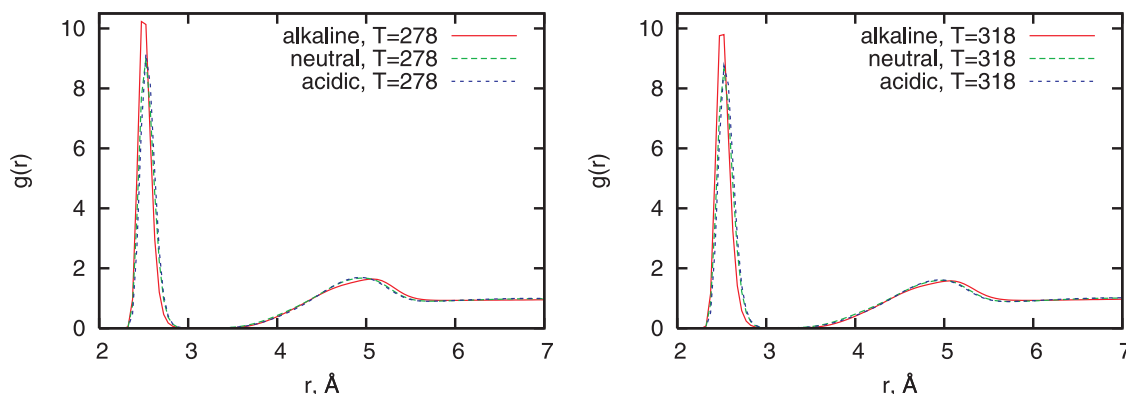


**Figure 1.** (Color online) The uranium-oxygen (of water and hydroxide ions) RDFs for  $T = 278$  K (left) and 318 K (right). Results for the alkaline solution are shown by solid red lines, neutral – by dashed green lines, and acidic – by dotted blue lines.

– for the neutral, and the blue dotted lines – for the acidic solutions. If one compares the RDFs between the two temperatures, it is clear that  $T = 278$  K case is characterized by the higher first peaks, indicating more stable formations under a lower temperature. One can also make another apparent observation: for both considered temperatures, extra  $\text{OH}^-$  ions in the solution favor the uranium-oxygen attraction while the neutral and acidic conditions demonstrate roughly the same weaker correlations. The roots of such a specific behavior in the alkaline case originate from a competition between  $\text{OH}^-$  ions and the water molecules to be bound to the uranyl ions. Since the hydroxide ions possess a negative charge, they are capable of pushing out the water molecules from the uranyl shell, occupying the vacancies and becoming preferential neighbors of the uranyles. To illustrate this fact, we show the uranium-hydrogen RDFs in figure 2. The distribution belonging to the alkaline case demonstrates the lower first peak reflecting a lack

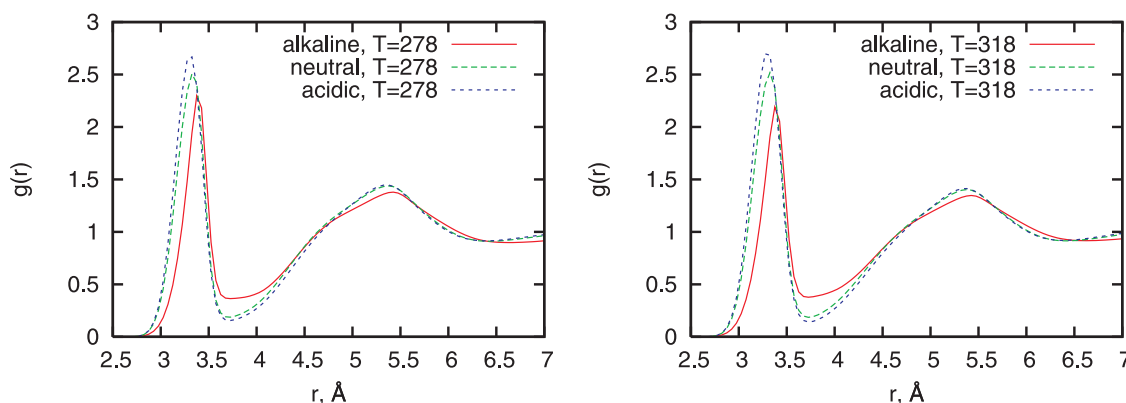


**Figure 2.** (Color online) The uranium-hydrogen (of water,  $\text{OH}^-$  and  $\text{H}^+$  ions) RDFs for  $T = 278$  K (left) and 318 K (right). The color scheme is the same as in figure 1.

of hydrogens in the uranyl hydration shell in comparison with the neutral and acidic solutions. Another consequence is the U–H peak shift toward larger distances since the O–H axis in the  $\text{OH}^-$  ions tends to be oriented directly from the uranium in contrast to water molecules. An acidic case yields the U–H peaks higher than the neutral peak due to extra  $\text{H}^+$  ions in the bulk, preventing the uranyl ligands from being hydrolyzed. A similar tendency to replace water molecules by  $\text{OH}^-$  ions and to keep the number of the ligands unchanged was previously found in [13].

Next we analyze the uranyl-uranyl coordination in terms of the uranium-uranium and the uranium-oxygen (of uranyl) RDFs. In figure 3 the U–U distributions for  $T = 278$  K and 318 K are presented. The

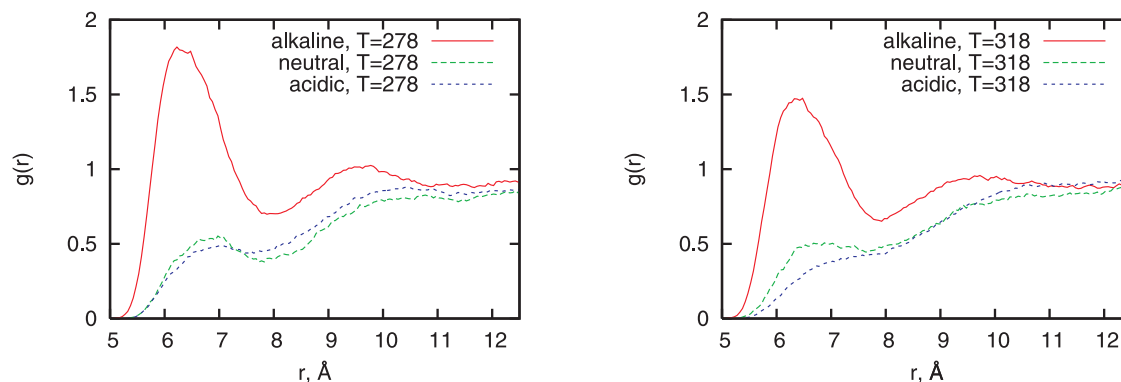


**Figure 3.** (Color online) The uranium-uranium RDFs for  $T = 278$  K (left) and 318 K (right). The color scheme is the same as in figure 1.

temperature effect follows the same pattern as the one observed for the uranyl-water correlation. Also, the neutral and the acidic cases behave similarly, while the alkaline one appears to differ from these two. Contrary to the neutral and the acidic solutions, one can see a prominent tendency for the uranyl-uranyl association in an alkaline solution. Such an intense uranyl correlation (attraction) in the alkaline solutions is a consequence of an increased screening of the uranils by  $\text{OH}^-$  ions and the attraction between the uranyl and shells (negatively charged by the hydroxide ions) of the other uranils. That is why the alkaline solution demonstrates the highest association ability in spite of a weaker association in the neutral and the acidic solutions.

Next we explore the correlation between the uranium and the oxygens of the uranils. In figure 4 the corresponding RDFs for  $T = 278$  K (left hand panel) and 318 K (right hand panel) are collected. As one can expect, the RDFs for the alkaline solution indicate a stronger correlation than the RDFs for the neutral and acidic cases. Nevertheless, all these RDFs show the peaks near 4.5–5.5 Å and 7–8 Å. Temperature produces a very similar effect by decreasing the peak heights.

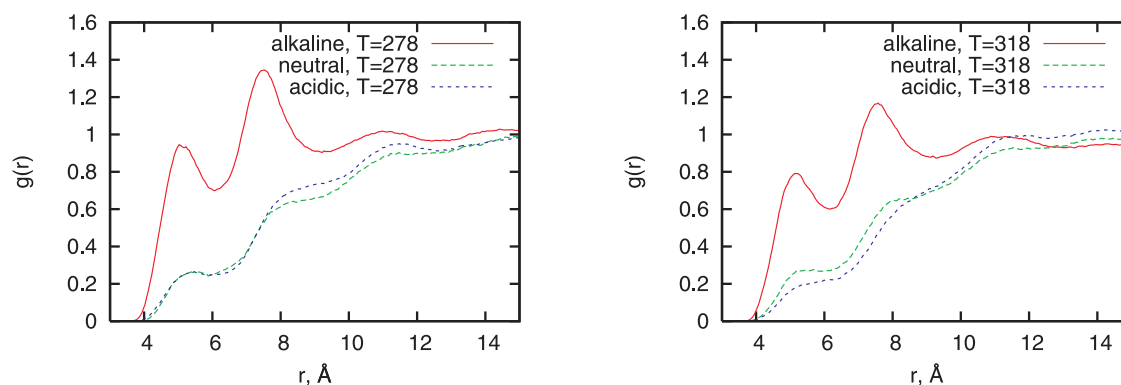


**Figure 4.** (Color online) The uranium-oxygen (of uranyl) RDFs for  $T = 278$  K (left) and 318 K (right). The color scheme is the same as in figure 1. Note that the intramolecular U=O bonds do not contribute to the RDFs shown.

One has to note that the RDFs in figures 3 and 4 are properly normalized and converge to unity at large distances but a shorter distance range is chosen in the plots to show the structural details.

### 3.2. Uranyl-uranyl mutual orientation

We made the angular analysis in order to clarify how the uranyles are mutually oriented being involved in the associates. During the simulation, the coordinates of the uranyles were stored and then processed. A straight and simple criterion to test whether the uranyles are forming an associate is the distance between uraniums: the location of the first minima of the U–U RDFs (figure 3) can be used for this purpose. Since the minima locations are smeared for different temperatures, a single distance threshold  $r = 7.5 \text{ \AA}$  was utilized. The angular analysis protocol is as follows: at every simulation step, one can assign a vector along the uranyl axis  $O=U=O$ . Next we consider a vector between two uranium ions when the distance between them is less than  $7.5 \text{ \AA}$ . A description of the mutual uranyl orientations can be treated in terms of two angles  $\alpha$ ,  $\beta$  between each of  $O=U=O$  axis and the U–U vector (see figure 5). The corresponding symmetrized probability distributions are shown in figure 6.

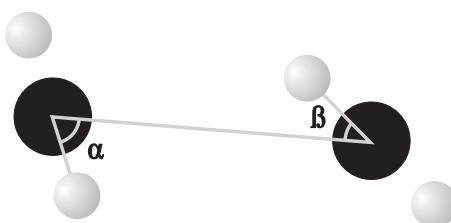


**Figure 5.** The uranyl-uranyl mutual orientation and characteristic angles.

As one can see from figure 6, the angular distributions show a pronounced dependence on pH of the solution, while the temperature effect is less apparent. We start with the acidic solutions: a bright spot in the symmetric range  $30\text{--}65^\circ$  indicates a configuration when both uranyles are tilted to the vector connecting the uraniums. A wide range of available angles speaks in favor of a “breathing” behavior of such associates. For a neutral solution at  $T = 278 \text{ K}$ , one can discriminate two probability spots at  $\alpha = 25\text{--}45^\circ$ ,  $\beta = 55\text{--}75^\circ$  and vice versa. At  $318 \text{ K}$ , the distribution demonstrates the similar shape though slightly smeared. The alkaline distribution for  $278 \text{ K}$  shows the symmetric spot at  $\alpha = \beta = 45\text{--}60^\circ$  with a tiny possibility for configurations with both angles equal to  $90^\circ$  (parallel orientation of uranyles). Similarly to the neutral case, the temperature makes a smearing effect when going to  $318 \text{ K}$ . One can see that the distributions for the alkaline solutions are characterized by more strict and localized spots. This is due to the hydroxide ions in the uranyl hydration shells when more electrostatic players take part in the stabilization of the polynuclear associate.

All the distributions indicate no associates with the arrangement of uranyles on a straight line (both angles are  $0^\circ$ ), and no associates with the perpendicular orientation (one angle is  $0^\circ$  and the other  $-90^\circ$ ).

### 3.3. Lifetimes and associate fractions

Apart from the structural information on the ordering of the uranyles in an associate, it is also interesting to measure the average time spent by them in the associated state. To obtain an information on the lifetimes of the uranyl associates, we monitor their trajectories during the simulation. Our strategy is: for any observed dimer (the distance between two uraniums is less than  $7.5 \text{ \AA}$ ) we start its individual “stopwatch” and let the stopwatch go during the time when the distance criterion remains satisfied. When an uranyl leaves an associate, the stopwatch is stopped. The actual procedure involves several steps: first (i), we determine the atom distributions and identify the uranyles involved in the associates ( $t = 0$ ), next (ii) we repeat this procedure (checking the configuration) every 5 elementary steps, that is on  $1.0 \text{ fs}$  interval. (iii) When the associate is broken ( $t = \tau$ ), we update the lifetime distribution  $f(\tau)$ . If another uranyl attaches to a dimer (the distance to any of dimer uraniums is less than  $7.5$ ), this associate becomes a trimer and a corresponding “stopwatch” is ascribed.

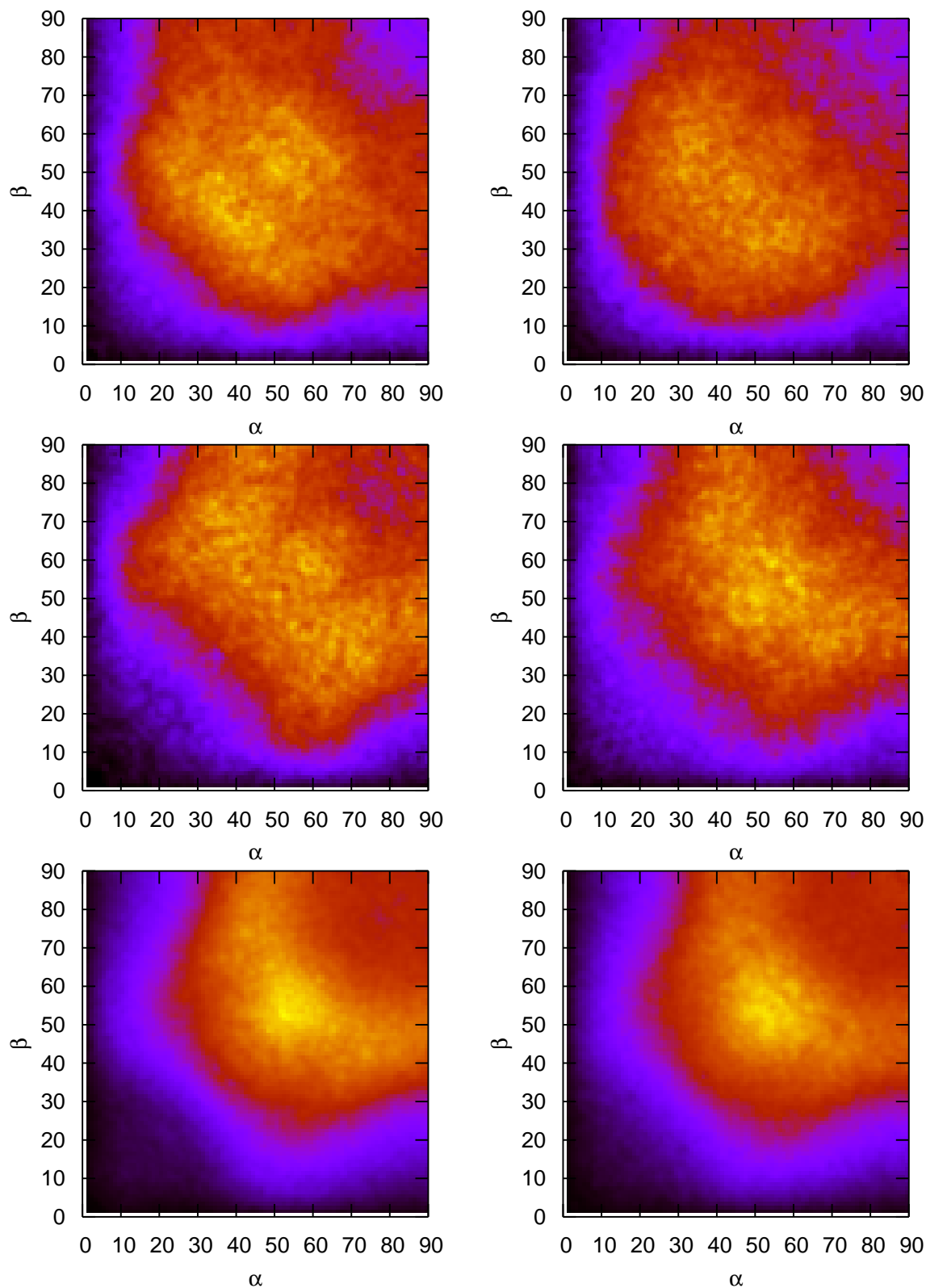


**Figure 6.** (Color online) The uranyl-uranyl angular distributions for the acidic (top), neutral (center) and alkaline (bottom row) solutions at  $T = 278$  K (left) and 318 K (right hand column). The colors correspond to the probability from low (dark) to high (bright) to find a corresponding configuration. Color scheme is scaled in such a way that the maximum values of all the distributions are of the same intensity.

Next, based on the lifetime distribution  $f(\tau)$ , we can estimate the average lifetimes as:

$$\langle \tau \rangle = \frac{\int_0^{\tau_{\max}} \tau f(\tau) d\tau}{\int_0^{\tau_{\max}} f(\tau) d\tau}, \quad (3.1)$$

where  $\tau_{\max} = 200$  ps is taken as the integration limit ( $\infty$ ) since the distributions  $f(\tau)$  have completely decayed at these times.

In table 2, we present the average lifetimes for the uranyl associates (dimers and trimers) at  $T = 278$  and 318 K. One can see that a decrease of the temperature extends the average lifetimes  $\langle \tau \rangle$ . Another factor favoring a formation of the associates is the presence of  $\text{OH}^-$  ions. That is why the strongest association uranyl capability is found for the alkaline solution at 278 K. As it was shown above, the association capability in the alkaline case is sufficiently increased due to the uranyl screening by the hydroxide ions. In the absence of  $\text{OH}^-$  ions, the acidic and neutral solutions behave in a similar way demonstrating a relatively close results within the uncertainties. Due to this, the lifetime for the acidic case at 278 K is longer than the one for the neutral case at 278 K. The average trimer lifetimes for the acidic case at 278 and 318 K do not fit the overall temperature tendency but the differences originate from the relatively short association events and do not change the main trends.

**Table 2.** The average lifetimes of the uranyl associates. Time units are – ps.

	dimers		trimers	
	278 K	318 K	278 K	318 K
acidic	14.18	5.71	1.84	2.55
neutral	13.79	6.21	3.15	2.65
alkaline	20.98	10.57	10.14	5.00

Sometimes [20, 21] in the studies of the association lifetimes, besides the distance criterion, the authors introduce an additional tolerance time. During this time, an associate is allowed to be broken and to be united back so that the lifetime “stopwatch” keeps running. The purpose of such a deployment is to avoid an overestimation of the shorter lifetimes due to sequent broken/united events. In our study we did not utilize this formalism because it is not well defined and does not affect the general conclusions.

Other quantities to consider are the fractions of the uranyls taking part in the formation of dimers and trimers. These fractions are defined as the number of the uranyls in the corresponding type of associates divided by the total number of the uranyls in the solution. The criteria for dimer and trimer creation events are the same as before. In table 3 the fractions are collected. As one can expect, the same tendencies can be found here as above for the average lifetimes: the low temperature and the presence of  $\text{OH}^-$  ions are the factors increasing the capability of the uranyls to associate.

**Table 3.** The fractions of the uranyls involved in the associates.

	dimers		trimers	
	278 K	318 K	278 K	318 K
acidic	0.132	0.077	0.008	0.006
neutral	0.154	0.133	0.019	0.023
alkaline	0.411	0.350	0.218	0.145

Despite the similar conclusions drawn from the lifetimes and the fractions, one has to note that the average lifetime does not contain the same information as the fraction of the associated uranyls: the same fraction of the associated uranyls can be obtained as a result of many short or, alternatively, fewer but longer (in time) formations.

## 4. Conclusions

The purpose of this study is to clarify in what way the temperature and pH effect the formation of the polynuclear associates in the uranyl aqueous solutions. For this purpose, we performed a series of MD simulations of the uranyl aqueous solutions at temperatures 278 and 318 K. To model different pH's the neutral system (containing waters and uranyls only) was mixed with the additional  $H^+$  or  $OH^-$  ions mimicking an acidic, or alkaline solutions. During the simulations we collected the necessary statistics on the radial distributions functions describing the uranyl hydration shells and the uranyl-uranyl correlation. Comparing the RDFs at the temperatures 278 and 318 K one can conclude that the increase of temperature leads to a decrease of the correlation (the peaks of the RDFs become lower). It is also found that in the acidic and the neutral solutions, the uranyl hydration shells stay unchanged, while in the alkaline case, the uranyls are preferably hydrated by the hydroxide ions. The modified hydration in the alkaline case results in the increased uranyl attraction contrary to a weak uranyl correlation in the neutral and the acidic solutions. The negatively charged  $OH^-$  ions screen the  $UO_2^{2+}$  ions allowing them to form more stable associates. In addition to the RDFs, we introduced the angular distributions reflecting the mutual orientation of the uranyls involved in the polynuclear associates. A temperature effect on the angular distributions is less apparent than the effect made by pH: indeed one can see that the distributions change the shape from smeared to a strict one when going from the acidic to the neutral and then to the alkaline case. This is due to the presence of the hydroxide ions in the uranyl hydration shells, that stabilize the uranyl-uranyl associates. For every solution we calculated the fraction of the uranyls taking part in the associates. Besides the fractions we also monitored the lifetimes of the uranyl dimers and trimers, built corresponding lifetime distributions, and extracted the average lifetimes for each case. The conclusions drawn agree with the ones from the RDFs: the low temperature and the alkaline environment are the factors favoring the long-lasting uranyl associates.

## Acknowledgements

The MD calculations were performed on the clusters of Ukrainian Academic Grid.



## References

1. Ahearne J.F., Phys. Today, 1997, **50**, 27; doi:10.1063/1.881763.
2. Spencer S., Gagliardi L., Handy N.C., Ioannou A.G., Skylaris C.-K., Willetts A., Simper A.M., J. Phys. Chem. A, 1999, **103**, 1831; doi:10.1021/jp983543s.
3. Tsushima S., Suzuki A., J. Mol. Struct. THEOCHEM, 2000, **529**, 21; doi:10.1016/S0166-1280(00)00526-1.
4. Liu C.X., Zachara J.M., Qafoku O., McKinley J.P., Headd S.M., Wang Z.W., Geochim. Cosmochim. Acta, 2004, **68**, 4519; doi:10.1016/j.gca.2004.04.017.
5. Guilbaud P., Wipff G., J. Phys. Chem., 1993, **97**, 5685; doi:10.1021/j100123a037.
6. Guilbaud P., Wipff G., J. Mol. Struct. THEOCHEM, 1996, **366**, 55; doi:10.1016/0166-1280(96)04496-X.
7. Greathouse J.A., O'Brien R.J., Bemis G., Pabalan R.T., J. Phys. Chem. B, 2002, **106**, 1646; doi:10.1021/jp013250q.
8. Nichols P., Bylaska E.J., Schenter G.K., de Jong W., J. Chem. Phys., 2008, **128**, 124507; doi:10.1063/1.2884861.
9. Holovko M.F., Kalyuzhnyi Yu.V., Druchok M.Yu., J. Phys. Stud., 2000, **4**, 100.
10. Druchok M.Yu., Bryk T.M., Holovko M.F., J. Phys. Stud., 2003, **7**, 402.
11. Holovko M., Druchok M., Bryk T., J. Chem. Phys., 2005, **123**, 154505; doi:10.1063/1.2064582.
12. Holovko M., Druchok M., Bryk T., J. Mol. Liq., 2007, **131–132**, 65; doi:10.1016/j.molliq.2006.08.029.
13. Holovko M., Druchok M., Bryk T., In: NATO Science for Peace and Security Series – A: Chemistry and Biology. Self-Organization of Molecular Systems, ed. by Russo N., Antonchenko V., Kryachko E., Springer, 2009, 221–253.
14. Nyberg A., Haymet A.D.J., In: Structure and Reactivity in Aqueous Solutions, ed. by Trular D., Kramer C., American Chem. Soc., New York, 1994.
15. Duh D.M., Perera D.N., Haymet A.D.J., J. Chem. Phys., 1995, **102**, 3736; doi:10.1063/1.468556.
16. Druchok M., Bryk T., Holovko M., J. Mol. Liq., 2005, **120**, 11; doi:10.1016/j.molliq.2004.07.071.
17. Ramsay J.D.F., In: Water and Aqueous Solutions, ed. by Neilson G.N., Enderby J.E., Adam Hilger, Bristol, 1986, p. 207.
18. Hayle J.M., Molecular Dynamics Simulations: Elementary Methods. Wiley, New York, 1992.
19. Melchionna S., Ciccotti G., Holian B.L., Mol. Phys., 1993, **78**, 533; doi:10.1080/00268979300100371.
20. Spohr E., In: Solid-Liquid Electrochemical Interfaces – ACS Symposium Series, ed. by Jerkiewicz G., Soriaga M.P., Uosaki K., Wieckowski A., American Chem. Soc., Washington DC, 1997, 31–44; doi:10.1021/bk-1997-0656.ch003.
21. Laage D., Hynes J.T., J. Phys. Chem. B, 2008, **112**, 7697; doi:10.1021/jp802033r.

## Вплив температури та рівня рН на асоціативність у водних розчинах уранілу

М. Дручок, М. Головко

Інститут фізики конденсованих систем НАН України, вул. Свенціцького 1, Львів 79011, Україна

Проведено дослідження процесів асоціативності у водних розчинах уранілу. Для цього проведено низку моделювань методом молекулярної динаміки. Під час моделювання проведено моніторинг фракцій іонів уранілу, що беруть участь у формуванні димерів та тримерів. Також зібрано розподіли імовірності за часами життя уранілових димерів та тримерів. Розглянуто вплив двох факторів – температури та рівня рН середовища – на здатність іонів уранілу до формування асоціатів. Виявлено, що збільшення температури знижує асоціативність, при цьому також скорочуються часи життя асоціатів і зменшуються фракції іонів уранілу у асоціатах. Вплив рівня рН середовища змодельовано додаванням іонів  $H^+$  чи  $OH^-$  до “нейтрального” розчину. Виявлено, що наявність у розчині іонів  $OH^-$  є сприятливим чинником для асоціативності, в той час як наявність іонів  $H^+$  призводить до протилежного ефекту. Для усіх розчинів проведено конфігураційний аналіз взаємної орієнтації іонів уранілу, що перебувають у асоціативному стані.

**Ключові слова:** молекулярна динаміка, водний розчин уранілу, асоціативність, рН, температура

---

---